The Distribution of Rectangular Patch Loads on Orthotropic Highway Bridge Decks

La répartition des charges concentrées (rectangulaires) sur les tabliers orthotropes des ponts pour routes principales

Die Verteilung von Radlasten auf orthotropen Brückenplatten

R. P. PAMA
Ph. D., Lecturer in Civil Engineering,
University of Dundee

A. R. CUSENS
Ph. D., Professor of Civil Engineering,
University of Dundee

Introduction

The development of new construction methods resulting in orthotropic structures especially in bridge construction has renewed interest in the problem of orthotropy. Although series solutions are available for the analysis of orthotropic plates and shells, slow convergence can make their use inconvenient even with the use of digital computers. It appears desirable to present an analysis for simple spans which avoids this major difficulty without sacrifice of accuracy in practical design.

The idealization of an actual structure of different rigidities in two orthogonal directions into an equivalent orthotropic plate on simple parallel supports is governed by the familiar equation

$$D_x \frac{\partial^4 w}{\partial x^4} + 2H \frac{\partial^4 w}{\partial x^2 \partial y^2} + D_y \frac{\partial^4 w}{\partial y^4} = p(x, y). \tag{1}$$

This is due to HUBER [1], and its application to bridge decks with negligible torsional rigidity ($H = 0$) was first introduced by GUYON [2] and later extended by MASSONNET [3] to cover all cases falling between the torsionless and isotropic cases. Hence it is apparent that the Guyon-Massonnet solutions are applicable only to those bridge deck where the square of half the total torsional rigidity does not exceed the product of the flexural rigidities in the two orthogonal directions ($H^2 \leqq D_x D_y$). In terms of Massonnet's parameter $\alpha = \frac{H}{\sqrt{D_x D_y}}$, the equations are valid only for $\alpha \leqq 1$. For bridge decks with

low flexural rigidities and for multi-cell bridge decks with high torsional rigidity, this condition may be exceeded and thus the Guyon-Massonnet solution is no longer valid. The authors [4, 5] have analyzed the case where $H^2 \geqq D_x D_y$ or (i.e. $\alpha \geqq 1$). Such bridge decks are designated torsionally stiff-flexurally soft to cover those cases falling between the extremes of the isotropix slab and the articulated deck ($D_y = 0$).

These analyses are for concentrated loads acting on the deck and as such are handicapped by the slow convergence of the series especially for moments, shears and reactive forces. Moreover, the use of concentrated loads to simulate the loads due to actual tyres is unrealistic since the actual live load imposed by traffic on a highway bridge is spread over an area, depending on vehicle weight, and tyre dimensions and inflation pressure. The loaded area of the bridge deck is larger than the contact area between the tyre and the roadway because of the load distributing action of the wearing surface, and depends upon its thickness and rigidity.

The use of rectangular patch loads to represent the tyre pressures on a bridge deck is realistic, and it will be shown that this approach overcomes the problem of convergence. Thus the evaluation of design parameters such as bending moment, becomes very convenient as it requires few harmonics of the series to give reasonable accuracy.

Theoretical Analysis

The effect of rectangular patch loads on simply supported orthotropic bridge decks may be obtained directly from the equation derived for concentrated load by integrating the function over a finite rectangular area. Using this method the analysis begins by considering a point load acting on the deck as has been done previously [4, 5].

The governing differential equation for a rectangular orthotropic plate is defined by Eq. (1) where the flexural rigidities per unit width in the x and y directions are D_x and D_y respectively and the torsional rigidity $2H$ is given by

$$2H = (D_{xy} + D_{yx} + D_1 + D_2), \tag{2}$$

where D_{xy} and D_{yx} are the torsional rigidities of the plate in the x and y directions respectively and D_1 and D_2 are the contributions of bending to the total torsional rigidity of the bridge deck. With these rigidities, the bending and torsional moments, shearing and reactive forces are functions of the deflection w as shown in Eq. (3).

$$\begin{aligned} M_x &= -\left(D_x \frac{\partial^2 w}{\partial x^2} + D_1 \frac{\partial^2 w}{\partial y^2}\right); & M_y &= -\left(D_y \frac{\partial^2 w}{\partial y^2} + D_2 \frac{\partial^2 w}{\partial x^2}\right); \\ M_{xy} &= D_{xy} \frac{\partial^2 w}{\partial x \, \partial y}; & M_{yx} &= -D_{yx} \frac{\partial^2 w}{\partial x \, \partial y}; \end{aligned} \tag{3}$$

$$
\begin{aligned}
V_x &= -\left[D_x \frac{\partial^3 w}{\partial x^3} + (D_{yx} + D_1) \frac{\partial^3 w}{\partial x \partial y^2}\right]; \\
V_y &= -\left[D_y \frac{\partial^3 w}{\partial y^3} + (D_{xy} + D_2) \frac{\partial^3 w}{\partial x^2 \partial y}\right]; \\
R_x &= -\left[D_x \frac{\partial^3 w}{\partial x^3} + (D_{yx} + D_{xy} + D_1) \frac{\partial^3 w}{\partial x \partial y^2}\right]; \\
R_y &= -\left[D_y \frac{\partial^3 w}{\partial y^3} + (D_{xy} + D_{yx} + D_2) \frac{\partial^3 w}{\partial x^2 \partial y}\right].
\end{aligned} \tag{3}
$$

The solution of the differential equation based on Levy's method may be classified into three distinct cases depending upon the relative rigidities of the deck. These are summarized as follows:

Case 1. $H^2 > D_x D_y$ (Special case $D_y = 0$)
Case 2. $H^2 = D_x D_y$
Case 3. $H^2 < D_x D_y$ (Special case $H = 0$)

Bridge decks within the first category have been classified by the authors [5] as torsionally stiff-flexurally soft bridge decks. These are characterized either by low flexural rigidity as in the multi-beam bridge deck with transverse shear connectors or by high torsional rigidity as in the multi-cell bridge decks. The solution of this particular case is based on the potitive roots of the characteristic equation.

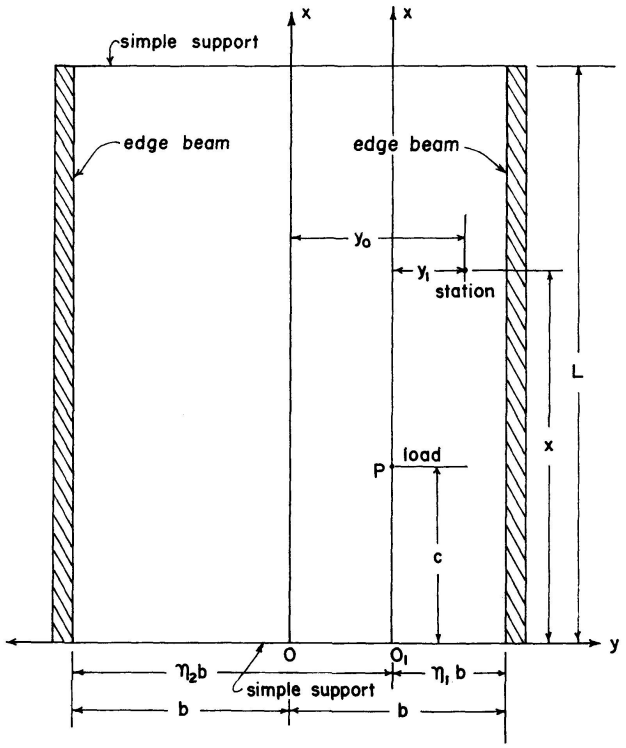

Fig. 1. Coordinate axes for point load acting on bridge deck.

The second category covers the familiar isotropic case where the flexural and torsional rigidities are equal. The solution may be employed for the analysis of uniform, solid slabs commonly encountered in practice.

The third and last category may be defined as torsionally soft-flexurally stiff bridge decks. These have a characteristically high flexural rigidity as compared with their torsional rigidity. Most composite bridge decks especially those of T-beam construction are under this case; the solution is based on the complex roots of the characteristic equation.

MASSONNET [3] has derived the expression for deflection for the second and third cases. The authors [4, 5] have previously analysed the first case for concentrated loads acting on the deck. It has been shown that for a concentrated load P acting at a distance c from the simple support as shown in Fig. 1, the equation for deflection at any point x may be written as

$$w = \frac{2PL^3}{\pi^4 D_x 2b} \sum_{n=1}^{\infty} \frac{1}{n^4} \operatorname{Sin} \alpha_n c \operatorname{Sin} \alpha_n x K_1, \tag{4}$$

where

$$\alpha_n = \frac{n\pi}{L} \tag{5}$$

and K_1 is a coefficient appropriate for each case written as K_{11}, K_{12} or K_{13} for cases 1, 2 or 3 respectively.

Considering now a wheel load W uniformly distributed over a rectangular area $2u \times 2v$ as shown in Fig. 2, the deflection function due to this finite

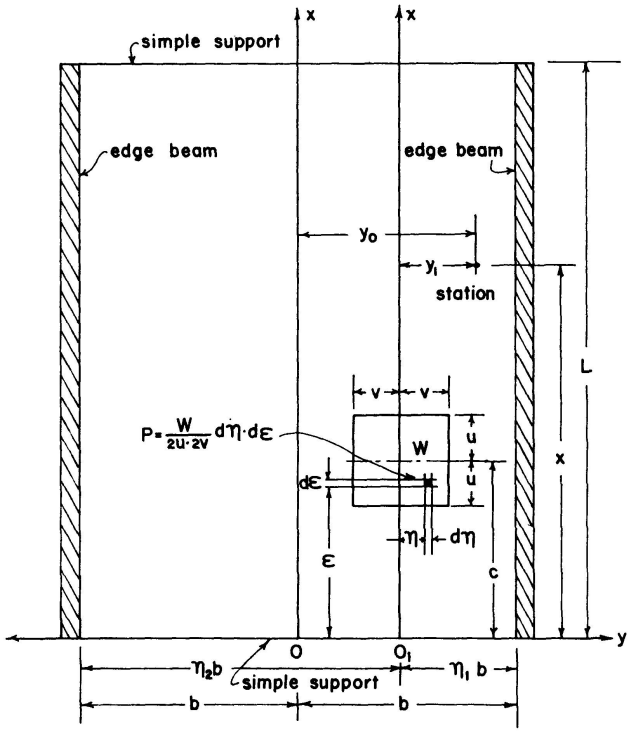

Fig. 2. Coordinate axes for rectangular patch load acting on bridge deck.

rectangular patch load is obtained by integrating the deflection from $(c-u)$ to $(c+u)$ along the x-axis and from $-v$ to $+v$ along the y-axis and the equation becomes

$$w = \frac{2\,W\,L^3}{2\,u\,2\,v\,\pi^4\,D_x\,2\,b}\sum_{n=1}^{\infty}\frac{1}{n^4}\operatorname{Sin}\alpha_n x\int_{c-u}^{c+u}\operatorname{Sin}\alpha_n \epsilon\, d\epsilon\,\frac{1}{2\,b}\int_{-v}^{v}K_1\,d\eta\,. \tag{6}$$

Setting

$$K_1^* = \frac{1}{2\,b}\int_{-v}^{v}K_1\,d\eta\,, \tag{7}$$

where K_1^* may be written as K_{11}^*, K_{12}^* or K_{13}^* as appropriate, the equation for deflection reduces to

$$w = \frac{W\,L^4}{u\,v\,\pi^5\,D_x}\sum_{n=1}^{\infty}\frac{1}{n^5}\operatorname{Sin}\alpha_n u\operatorname{Sin}\alpha_n c\operatorname{Sin}\alpha_n x\,(K_1^*)\,. \tag{8}$$

With the expression for deflection known, the moments, shears and reactive forces due to a rectangular patch load are obtained by successive differentiation and these are summarized as follows:

Case 1. Torsionally Stiff-Flexurally Soft Bridge Decks
$(H^2 \geqq D_x D_y\,;\,\alpha \geqq 1)$

Deflection:

$$w = \frac{W\,L^4}{u\,v\,\pi^5\,D_x}\sum_{n=1}^{\infty}\frac{1}{n^5}\operatorname{Sin}\alpha_n u\operatorname{Sin}\alpha_n c\operatorname{Sin}\alpha_n x\,(K_{11}^*)\,. \tag{8a}$$

Longitudinal Moment:

$$M_x = \frac{W\,L^2}{u\,v\,\pi^3}\sum_{n=1}^{\infty}\frac{1}{n^3}\operatorname{Sin}\alpha_n u\operatorname{Sin}\alpha_n c\operatorname{Sin}\alpha_n x\left(K_{11}^* - \frac{D_1}{D_x}K_{21}^*\right). \tag{9}$$

Transverse Moment:

$$M_y = -\frac{W\,L^2}{u\,v\,\pi^3}\sum_{n=1}^{\infty}\frac{1}{n^3}\operatorname{Sin}\alpha_n u\operatorname{Sin}\alpha_n c\operatorname{Sin}\alpha_n x\left(\frac{D_y}{D_x}K_{21}^* - \frac{D_2}{D_x}K_{11}^*\right). \tag{10}$$

Longitudinal Twist:

$$M_{xy} = \frac{W\,L^2}{u\,v\,\pi^3}\sum_{n=1}^{\infty}\frac{1}{n^3}\operatorname{Sin}\alpha_n u\operatorname{Sin}\alpha_n c\operatorname{Cos}\alpha_n x\left(\frac{D_{xy}}{D_y}K_{31}^*\right). \tag{11}$$

Transverse Twist:

$$M_{yx} = -\frac{W\,L^2}{u\,v\,\pi^3}\sum_{n=1}^{\infty}\frac{1}{n^3}\operatorname{Sin}\alpha_n u\operatorname{Sin}\alpha_n c\operatorname{Cos}\alpha_n x\left(\frac{D_{yx}}{D_y}K_{31}^*\right). \tag{12}$$

Longitudinal Shear:

$$V_x = \frac{W L}{u v \pi^2} \sum_{n=1}^{\infty} \frac{1}{n^2} \operatorname{Sin} \alpha_n u \operatorname{Sin} \alpha_n c \operatorname{Cos} \alpha_n x \left[K_{11}^* - \left(\frac{D_{yx} + D_1}{D_x} \right) K_{21}^* \right]. \tag{13}$$

Transverse Shear:

$$V_y = \frac{W L}{u v \pi^2} \sum_{n=1}^{\infty} \frac{1}{n^2} \operatorname{Sin} \alpha_n u \operatorname{Sin} \alpha_n c \operatorname{Sin} \alpha_n x \left[K_{41}^* - \left(\frac{D_2 + D_{xy}}{D_y} \right) K_{31}^* \right]. \tag{14}$$

Longitudinal Reactive Force:

$$R_x = \frac{W L}{u v \pi^2} \sum_{n=1}^{\infty} \frac{1}{n^2} \operatorname{Sin} \alpha_n u \operatorname{Sin} \alpha_n c \operatorname{Cos} \alpha_n x \left[K_{11}^* - \left(\frac{D_{xy} + D_{yx} + D_1}{D_x} \right) K_{21}^* \right]. \tag{15}$$

Transverse Reactive Force:

$$R_y = -\frac{W L}{u v \pi^2} \sum_{n=1}^{\infty} \frac{1}{n^2} \operatorname{Sin} \alpha_n u \operatorname{Sin} \alpha_n c \operatorname{Sin} \alpha_n x \left[K_{41}^* - \left(\frac{D_{xy} + D_{yx} + D_2}{D_y} \right) K_{31}^* \right]. \tag{16}$$

Setting

$$r_1 = \sqrt{\frac{H}{D_y} + \sqrt{\left(\frac{H}{D_y} \right)^2 - \frac{D_x}{D_y}}} \tag{17}$$

and

$$r_2 = \sqrt{\frac{H}{D_y} - \sqrt{\left(\frac{H}{D_y} \right)^2 - \frac{D_x}{D_y}}} \tag{18}$$

the dimensionless terms K_{11}^*, K_{21}^*, K_{31}^* and K_{41}^* are defined as follows:

For $\xi_1 \lesseqgtr \psi$

$$K_{11}^* = \frac{D_x}{2 D_y (r_1^2 - r_2^2)} \left[\frac{1}{r_2^2} (e^{-\beta_2(\xi_1 - \psi)} - e^{-\beta_2(\xi_1 + \psi)}) - \frac{1}{r_1^2} (e^{-\beta_1(\xi_1 - \psi)} - e^{-\beta_1(\xi_1 + \psi)}) \right.$$
$$\left. + A_n^* \operatorname{Cosh} \beta_1 \xi_0 + B_n^* \operatorname{Cosh} \beta_2 \xi_0 + C_n^* \operatorname{Sinh} \beta_1 \xi_0 + D_n^* \operatorname{Sinh} \beta_2 \xi_0 \right], \tag{19}$$

$$K_{21}^* = \frac{D_x}{2 D_y (r_1^2 - r_2^2)} [(e^{-\beta_2(\xi_1 - \psi)} - e^{-\beta_2(\xi_1 + \psi)}) - (e^{-\beta_1(\xi_1 - \psi)} - e^{-\beta_1(\xi_1 + \psi)})$$
$$+ r_1^2 A_n^* \operatorname{Cosh} \beta_1 \xi_0 + r_2^2 B_n^* \operatorname{Cosh} \beta_2 \xi_0 + r_1^2 C_n^* \operatorname{Sinh} \beta_1 \xi_0 + r_2^2 D_n^* \operatorname{Sinh} \beta_2 \xi_0], \tag{20}$$

$$K_{31}^* = \frac{1}{2 (r_1^2 - r_2^2)} \left[\pm \left\{ \frac{1}{r_1} (e^{-\beta_1(\xi_1 - \psi)} - e^{-\beta_1(\xi_1 + \psi)}) - \frac{1}{r_2} (e^{-\beta_2(\xi_1 - \psi)} - e^{-\beta_2(\xi_1 + \psi)}) \right\} \right.$$
$$\left. + r_1 A_n^* \operatorname{Sinh} \beta_1 \xi_0 + r_2 B_n^* \operatorname{Sinh} \beta_2 \xi_0 + r_1 C_n^* \operatorname{Cosh} \beta_1 \xi_0 + r_2 D_n^* \operatorname{Cosh} \beta_2 \xi_0 \right], \tag{21}$$

$$K_{41}^* = \frac{1}{2 (r_1^2 - r_2^2)} [\pm \{ r_1 (e^{-\beta_1(\xi_1 - \psi)} - e^{-\beta_1(\xi_1 + \psi)}) - r_2 (e^{-\beta_2(\xi_1 - \psi)} - e^{-\beta_2(\xi_1 + \psi)}) \}$$
$$+ r_1^3 A_n^* \operatorname{Sinh} \beta_1 \xi_0 + r_2^3 B_n^* \operatorname{Sinh} \beta_2 \xi_0 + r_1^3 C_n^* \operatorname{Cosh} \beta_1 \xi_0 + r_2^3 D_n^* \operatorname{Cosh} \beta_2 \xi_0]. \tag{22}$$

The expressions for stations at the centre of the load where $\xi_1 = 0$, are obtained by setting ξ_1 and ψ equal to $\psi/2$ and doubling the result. This is done for the particular solution only and following this, the equations for K_{11}^*, K_{21}^*, K_{31}^* and K_{41}^* are as follows:

For $\xi_1 = 0$

$$K_{11}^* = \frac{D_x}{2D_y(r_1^2-r_2^2)}\left[\frac{2}{r_2^2}(1-e^{-\beta_2\psi})-\frac{2}{r_1^2}(1-e^{-\beta_1\psi})\right.$$
$$\left.+A_n^*\operatorname{Cosh}\beta_1\xi_0+B_n^*\operatorname{Cosh}\beta_2\xi_0+C_n^*\operatorname{Sinh}\beta_1\xi_0+D_n^*\operatorname{Sinh}\beta_2\xi_0\right], \tag{23}$$

$$K_{21}^* = \frac{D_x}{2D_y(r_1^2-r_2^2)}[2(e^{-\beta_1\psi}-e^{-\beta_2\psi})$$
$$+r_1^2A_n^*\operatorname{Cosh}\beta_1\xi_0+r_2^2B_n^*\operatorname{Cosh}\beta_2\xi_0+r_1^2C_n^*\operatorname{Sinh}\beta_1\xi_0+r_2^2D_n^*\operatorname{Sinh}\beta_2\xi_0], \tag{24}$$

$$K_{31}^* = \frac{1}{2(r_1^2-r_2^2)}[+r_1A_n^*\operatorname{Sinh}\beta_1\xi_0+r_2B_n^*\operatorname{Sinh}\beta_2\xi_0$$
$$+r_1C_n^*\operatorname{Cosh}\beta_1\xi_0+r_2D_n^*\operatorname{Cosh}\beta_2\xi_0], \tag{25}$$

$$K_{41}^* = \frac{1}{2(r_1^2-r_2^2)}[+r_1^3A_n^*\operatorname{Sinh}\beta_1\xi_0+r_2^3B_n^*\operatorname{Sinh}\beta_2\xi_0$$
$$+r_1^3C_n^*\operatorname{Cosh}\beta_1\xi_0+r_2^3D_n^*\operatorname{Cosh}\beta_2\xi_0]. \tag{26}$$

The positive and negative signs used for K_{31}^* and K_{41}^* are for station to the right and left of the load respectively.

The constants used are defined as follows:

$$A_n^* = \frac{(S_{31}^*-S_{41}^*)b_{11}-(S_{11}^*+S_{21}^*)b_{31}}{2(a_{31}b_{11}-a_{11}b_{31})}, \tag{27a}$$

$$B_n^* = \frac{(S_{11}^*+S_{21}^*)a_{31}-(S_{31}^*-S_{41}^*)a_{11}}{2(a_{31}b_{11}-a_{11}b_{31})}, \tag{27b}$$

$$C_n^* = \frac{(S_{31}^*+S_{41}^*)d_{11}-(S_{11}^*-S_{21}^*)d_{31}}{2(c_{31}d_{11}-c_{11}d_{31})}, \tag{27c}$$

$$D_n^* = \frac{(S_{11}^*-S_{21}^*)c_{31}-(S_{31}^*+S_{41}^*)c_{11}}{2(c_{31}d_{11}-c_{11}d_{31})}, \tag{27d}$$

where

$$S_{11}^* = \frac{1}{r_1}\left[GJ\alpha_n+(D_yr_1^2-D_2)\frac{1}{r_1}\right][e^{-\beta_1(\eta_1-\psi)}-e^{-\beta_1(\eta_1+\psi)}]$$
$$-\frac{1}{r_2}\left[GJ\alpha_n+(D_yr_2^2-D_2)\frac{1}{r_2}\right][e^{-\beta_2(\eta_1-\psi)}-e^{-\beta_2(\eta_1+\psi)}], \tag{28a}$$

$$S_{21}^* = \frac{1}{r_1}\left[GJ\alpha_n+(D_yr_1^2-D_2)\frac{1}{r_1}\right][e^{-\beta_1(\eta_2-\psi)}-e^{-\beta_1(\eta_2+\psi)}]$$
$$-\frac{1}{r_2}\left[GJ\alpha_n+(D_yr_2^2-D_2)\frac{1}{r_2}\right][e^{-\beta_2(\eta_2-\psi)}-e^{-\beta_2(\eta_2+\psi)}], \tag{28b}$$

$$S_{31}^* = \frac{1}{r_1^2}[EI\alpha_n+(D_yr_1^2-D_2-D_{xy}-D_{yx})r_1][e^{-\beta_1(\eta_1-\psi)}-e^{-\beta_1(\eta_1+\psi)}]$$
$$-\frac{1}{r_2^2}[EI\alpha_n+(D_yr_2^2-D_2-D_{xy}-D_{yx})r_2][e^{-\beta_2(\eta_1-\psi)}-e^{-\beta_2(\eta_1+\psi)}], \tag{28c}$$

$$S_{41}^{*} = -\frac{1}{r_1^2}[E\,I\,\alpha_n + (D_y r_1^2 - D_2 - D_{xy} - D_{yx})\,r_1]\,[e^{-\beta_1(\eta_2-\psi)} - e^{-\beta_1(\eta_2+\psi)}]$$
$$+\frac{1}{r_2^2}[E\,I\,\alpha_n + (D_y r_2^2 - D_2 - D_{xy} - D_{yx})\,r_2]\,[e^{-\beta_2(\eta_2-\psi)} - e^{-\beta_2(\eta_2+\psi)}] \tag{28d}$$

and the terms $a_{11}, b_{11} \ldots d_{31}$ are given by the following:

$$a_{11} = (D_y r_1^2 - D_2)\,\mathrm{Cosh}\,\beta_1 - G\,J\,\alpha_n r_1\,\mathrm{Sinh}\,\beta_1, \tag{29a}$$
$$b_{11} = (D_y r_2^2 - D_2)\,\mathrm{Cosh}\,\beta_2 - G\,J\,\alpha_n r_2\,\mathrm{Sinh}\,\beta_2, \tag{29b}$$
$$c_{11} = (D_y r_1^2 - D_2)\,\mathrm{Sinh}\,\beta_1 - G\,J\,\alpha_n r_1\,\mathrm{Cosh}\,\beta_1, \tag{29c}$$
$$d_{11} = (D_y r_2^2 - D_2)\,\mathrm{Sinh}\,\beta_2 - G\,J\,\alpha_n r_2\,\mathrm{Cosh}\,\beta_2, \tag{29d}$$
$$a_{31} = E\,I\,\alpha_n\,\mathrm{Cosh}\,\beta_1 - r_1(D_y r_1^2 - D_2 - D_{xy} - D_{yx})\,\mathrm{Sinh}\,\beta_1, \tag{29e}$$
$$b_{31} = E\,I\,\alpha_n\,\mathrm{Cosh}\,\beta_2 - r_2(D_y r_2^2 - D_2 - D_{xy} - D_{yx})\,\mathrm{Sinh}\,\beta_2, \tag{29f}$$
$$c_{31} = E\,I\,\alpha_n\,\mathrm{Sinh}\,\beta_1 - r_1(D_y r_1^2 - D_2 - D_{xy} - D_{yx})\,\mathrm{Cosh}\,\beta_1, \tag{29g}$$
$$d_{31} = E\,I\,\alpha_n\,\mathrm{Sinh}\,\beta_2 - r_2(D_y r_2^2 - D_2 - D_{xy} - D_{yx})\,\mathrm{Cosh}\,\beta_2. \tag{29h}$$

The dimensionless parameters β_1 and β_2 are defined as follows:

$$\beta_1 = \alpha_n b\,r_1 = \frac{n\pi b}{L}\sqrt{\frac{H}{D_y} + \sqrt{\left(\frac{H}{D_y}\right)^2 - \frac{D_x}{D_y}}}, \tag{30}$$

$$\beta_2 = \alpha_n b\,r_2 = \frac{n\pi b}{L}\sqrt{\frac{H}{D_y} - \sqrt{\left(\frac{H}{D_y}\right)^2 - \frac{D_x}{D_y}}}. \tag{31}$$

The location of the station relative to the centre of the bridge and load respectively are given by

$$\xi_0 = \frac{y_0}{b} \tag{32}$$

and

$$\xi_1 = Abs\left[\frac{y_1}{b}\right]. \tag{33}$$

Referring to Fig. 2, ξ_1 may be conveniently written as

$$\xi_1 = Abs\,[1 + \xi_0 - \eta_2]. \tag{34}$$

The width of the patch load relative to the width of the bridge is given by ψ, thus

$$\psi = v/b. \tag{35}$$

Case 3. Torsionally Soft-Flexurally Stiff Bridge Decks
$(H^2 \leqq D_x D_y;\ \alpha \leqq 1)$

Most orthotropic bridge decks will be in this category and following the same procedure as was done for case 1, the following equations are obtained for deflection, moments, shears and reactive forces.

Deflection:

$$w = \frac{W L^4}{u v \pi^5 D_x} \sum_{n=1}^{\infty} \frac{1}{n^5} \operatorname{Sin} \alpha_n u \operatorname{Sin} \alpha_n c \operatorname{Sin} \alpha_n x \, (K_{13}^*). \tag{36}$$

Longitudinal Moment:

$$M_x = \frac{W L^2}{u v \pi^3} \sum_{n=1}^{\infty} \frac{1}{n^3} \operatorname{Sin} \alpha_n u \operatorname{Sin} \alpha_n c \operatorname{Sin} \alpha_n x \left(K_{13}^* - \frac{D_1}{D_x} K_{23}^* \right). \tag{37}$$

Transverse Moment:

$$M_y = -\frac{W L^2}{u v \pi^3} \sum_{n=1}^{\infty} \frac{1}{n^3} \operatorname{Sin} \alpha_n u \operatorname{Sin} \alpha_n c \operatorname{Sin} \alpha_n x \left(\frac{D_y}{D_x} K_{23}^* - \frac{D_2}{D_x} K_{13}^* \right). \tag{38}$$

Longitudinal Twisting Moment:

$$M_{xy} = \frac{W L^2}{u v \pi^3} \sum_{n=1}^{\infty} \frac{1}{n^3} \operatorname{Sin} \alpha_n u \operatorname{Sin} \alpha_n c \operatorname{Cos} \alpha_n x \left(\frac{D_{xy}}{D_y} K_{33}^* \right). \tag{39}$$

Transverse Twisting Moment:

$$M_{yx} = -\frac{W L^2}{u v \pi^3} \sum_{n=1}^{\infty} \frac{1}{n^3} \operatorname{Sin} \alpha_n u \operatorname{Sin} \alpha_n c \operatorname{Cos} \alpha_n x \left(\frac{D_{yx}}{D_y} K_{33}^* \right). \tag{40}$$

Longitudinal Shear:

$$V_x = \frac{W L}{u v \pi^2} \sum_{n=1}^{\infty} \frac{1}{n^2} \operatorname{Sin} \alpha_n u \operatorname{Sin} \alpha_n c \operatorname{Cos} \alpha_n x \left(K_{13}^* - \frac{D_1 + D_{yx}}{D_x} K_{23}^* \right). \tag{41}$$

Transverse Shear:

$$V_y = -\frac{W L}{u v \pi^2} \sum_{n=1}^{\infty} \frac{1}{n^2} \operatorname{Sin} \alpha_n u \operatorname{Sin} \alpha_n c \operatorname{Sin} \alpha_n x \left(K_{43}^* - \frac{D_2 + D_{xy}}{D_y} K_{33}^* \right). \tag{42}$$

Longitudinal Reactive Force:

$$R_x = \frac{W L}{u v \pi^2} \sum_{n=1}^{\infty} \frac{1}{n^2} \operatorname{Sin} \alpha_n u \operatorname{Sin} \alpha_n c \operatorname{Cos} \alpha_n x \left(K_{13}^* - \frac{D_1 + D_{xy} + D_{yx}}{D_x} K_{23}^* \right). \tag{43}$$

Transverse Reactive Force:

$$R_y = -\frac{W L}{u v \pi^2} \sum_{n=1}^{\infty} \frac{1}{n^2} \operatorname{Sin} \alpha_n u \operatorname{Sin} \alpha_n c \operatorname{Sin} \alpha_n x \left(K_{43}^* - \frac{D_2 + D_{xy} + D_{yx}}{D_y} K_{33}^* \right). \tag{44}$$

With

$$r_3 = \sqrt{\frac{\sqrt{\frac{D_x}{D_y}} + \frac{H}{D_y}}{2}} \tag{45}$$

and

$$r_4 = \sqrt{\frac{\sqrt{\frac{D_x}{D_y}} - \frac{H}{D_y}}{2}} \tag{46}$$

the coefficients K_{13}^*, K_{23}^*, K_{33}^* and K_{43}^* may be defined as follows:

For $\xi_1 \lesseqgtr \psi$

$$\begin{aligned}K_{13}^* = \frac{D_x}{4 D_y r_3 r_4}\Bigg[&\frac{1}{(r_3^2+r_4^2)^2}\{[2 r_3 r_4 \operatorname{Cos}\beta_4(\xi_1-\psi)+(r_3^2-r_4^2)\operatorname{Sin}\beta_4(\xi_1-\psi)]\, e^{-\beta_3(\xi_1-\psi)}\\ &-[2 r_3 r_4 \operatorname{Cos}\beta_4(\xi_1+\psi)+(r_3^2-r_4^2)\operatorname{Sin}\beta_4(\xi_1+\psi)]\, e^{-\beta_3(\xi_1+\psi)}\}\\ &+A_m^*\operatorname{Cosh}\beta_3\xi_0\operatorname{Cos}\beta_4\xi_0+B_m^*\operatorname{Cosh}\beta_3\xi_0\operatorname{Sin}\beta_4\xi_0\\ &+C_m^*\operatorname{Sinh}\beta_3\xi_0\operatorname{Cos}\beta_4\xi_0+D_m^*\operatorname{Sinh}\beta_3\xi_0\operatorname{Sin}\beta_4\xi_0\Bigg],\end{aligned} \tag{47}$$

$$\begin{aligned}K_{23}^* = \frac{D_x}{4 D_y r_3 r_4}[&\{\operatorname{Sin}\beta_4(\xi_1-\psi)\, e^{-\beta_3(\xi_1-\psi)}-\operatorname{Sin}\beta_4(\xi_1+\psi)\, e^{-\beta_3(\xi_1+\psi)}\}\\ &+A_m^*\{(r_3^2-r_4^2)\operatorname{Cosh}\beta_3\xi_0\operatorname{Cos}\beta_4\xi_0-2 r_3 r_4\operatorname{Sinh}\beta_3\xi_0\operatorname{Sin}\beta_4\xi_0\}\\ &+B_m^*\{(r_3^2-r_4^2)\operatorname{Cosh}\beta_3\xi_0\operatorname{Sin}\beta_4\xi_0+2 r_3 r_4\operatorname{Sinh}\beta_3\xi_0\operatorname{Cos}\beta_4\xi_0\}\\ &+C_m^*\{(r_3^2-r_4^2)\operatorname{Sinh}\beta_3\xi_0\operatorname{Cos}\beta_4\xi_0-2 r_3 r_4\operatorname{Cosh}\beta_3\xi_0\operatorname{Sin}\beta_4\xi_0\}\\ &+D_m^*\{(r_3^2-r_4^2)\operatorname{Sinh}\beta_3\xi_0\operatorname{Sin}\beta_4\xi_0+2 r_3 r_4\operatorname{Cosh}\beta_3\xi_0\operatorname{Cos}\beta_4\xi_0\}],\end{aligned} \tag{48}$$

$$\begin{aligned}K_{33}^* = \frac{1}{4 r_3 r_4}\Bigg[&\frac{\pm 1}{(r_3^2+r_4^2)}\{[r_3\operatorname{Sin}\beta_4(\xi_1+\psi)+r_4\operatorname{Cos}\beta_4(\xi_1+\psi)]\, e^{-\beta_3(\xi_1+\psi)}\\ &-[r_3\operatorname{Sin}\beta_4(\xi_1-\psi)+r_4\operatorname{Cos}\beta_4(\xi_1-\psi)]\, e^{-\beta_3(\xi_1-\psi)}\}\\ &+A_m^*\{r_3\operatorname{Sinh}\beta_3\xi_0\operatorname{Cos}\beta_4\xi_0-r_4\operatorname{Cosh}\beta_3\xi_0\operatorname{Sin}\beta_4\xi_0\}\\ &+B_m^*\{r_3\operatorname{Sinh}\beta_3\xi_0\operatorname{Sin}\beta_4\xi_0+r_4\operatorname{Cosh}\beta_3\xi_0\operatorname{Cos}\beta_4\xi_0\}\\ &+C_m^*\{r_3\operatorname{Cosh}\beta_3\xi_0\operatorname{Cos}\beta_4\xi_0-r_4\operatorname{Sinh}\beta_3\xi_0\operatorname{Sin}\beta_4\xi_0\}\\ &+D_m^*\{r_3\operatorname{Cosh}\beta_3\xi_0\operatorname{Sin}\beta_4\xi_0+r_4\operatorname{Sinh}\beta_3\xi_0\operatorname{Cos}\beta_4\xi_0\}\Bigg],\end{aligned} \tag{49}$$

and

$$\begin{aligned}K_{43}^* = \frac{1}{4 r_3 r_4}[&\pm\{[r_4\operatorname{Cos}\beta_4(\xi_1-\psi)-r_3\operatorname{Sin}\beta_4(\xi_1-\psi)]\, e^{-\beta_3(\xi_1-\psi)}\\ &-[r_4\operatorname{Cos}\beta_4(\xi_1+\psi)-r_3\operatorname{Sin}\beta_4(\xi_1+\psi)\, e^{-\beta_3(\xi_1+\psi)}\}\\ &+A_m^*\{(r_3^3-3 r_3 r_4^2)\operatorname{Sinh}\beta_3\xi_0\operatorname{Cos}\beta_4\xi_0+(r_4^3-3 r_4 r_3^2)\operatorname{Cosh}\beta_3\xi_0\operatorname{Sin}\beta_4\xi_0\}\\ &+B_m^*\{(r_3^3-3 r_3 r_4^2)\operatorname{Sinh}\beta_3\xi_0\operatorname{Sin}\beta_4\xi_0-(r_4^3-3 r_4 r_3^2)\operatorname{Cosh}\beta_3\xi_0\operatorname{Cos}\beta_4\xi_0\}\\ &+C_m^*\{(r_3^3-3 r_3 r_4^2)\operatorname{Cosh}\beta_3\xi_0\operatorname{Cos}\beta_4\xi_0+(r_4^3-3 r_4 r_3^2)\operatorname{Sinh}\beta_3\xi_0\operatorname{Sin}\beta_4\xi_0\}\\ &+D_m^*\{(r_3^3-3 r_3 r_4^2)\operatorname{Cosh}\beta_3\xi_0\operatorname{Sin}\beta_4\xi_0-(r_4^3-3 r_4 r_3^2)\operatorname{Sinh}\beta_3\xi_0\operatorname{Cos}\beta_4\xi_0\}].\end{aligned} \tag{50}$$

Eqs. (47–50) are valid for $\xi_1 \lesseqgtr \psi$ and special expressions for stations under the centre of the load defined by $\xi_1 = 0$ may be derived following the same procedure adopted for Case 1. This is achieved by substituting $\psi/2$ for ξ_1 and ψ and doubling the results for the particular solution only, and following this, the coefficient K_{13}^*, K_{23}^*, K_{33}^* and K_{43}^* for $\xi_1 = 0$ are as follows:

For $\xi_1 = 0$

$$K_{13}^* = \frac{D_x}{4 D_y r_3 r_4}\left[\frac{2}{(r_3^2+r_4^2)^2}\{2 r_3 r_4 - [2 r_3 r_4 \operatorname{Cos}\beta_4\psi + (r_3^2 - r_4^2)\operatorname{Sin}\beta_4\psi]e^{-\beta_3\psi}\}\right.$$
$$+ A_m^* \operatorname{Cosh}\beta_3\xi_0 \operatorname{Cos}\beta_4\xi_0 + B_m^* \operatorname{Cosh}\beta_3\xi_0 \operatorname{Sin}\beta_4\xi_0 \tag{51}$$
$$\left. + C_m^* \operatorname{Sinh}\beta_3\xi_0 \operatorname{Cos}\beta_4\xi_0 + D_m^* \operatorname{Sinh}\beta_3\xi_0 \operatorname{Sin}\beta_4\xi_0\right],$$

$$K_{23}^* = \frac{D_x}{4 D_y r_3 r_4}[(-2\operatorname{Sin}\beta_4\psi)\, e^{-\beta_3\psi}$$
$$+ A_m^*\{(r_3^2 - r_4^2)\operatorname{Cosh}\beta_3\xi_0 \operatorname{Cos}\beta_4\xi_0 - 2 r_3 r_4 \operatorname{Sinh}\beta_3\xi_0 \operatorname{Sin}\beta_4\xi_0\}$$
$$+ B_m^*\{(r_3^2 - r_4^2)\operatorname{Cosh}\beta_3\xi_0 \operatorname{Sin}\beta_4\xi_0 + 2 r_3 r_4 \operatorname{Sinh}\beta_3\xi_0 \operatorname{Cos}\beta_4\xi_0\} \tag{52}$$
$$+ C_m^*\{(r_3^2 - r_4^2)\operatorname{Sinh}\beta_3\xi_0 \operatorname{Cos}\beta_4\xi_0 - 2 r_3 r_4 \operatorname{Cosh}\beta_3\xi_0 \operatorname{Sin}\beta_4\xi_0\}$$
$$+ D_m^*\{(r_3^2 - r_4^2)\operatorname{Sinh}\beta_3\xi_0 \operatorname{Sin}\beta_4\xi_0 + 2 r_3 r_4 \operatorname{Cosh}\beta_3\xi_0 \operatorname{Cos}\beta_4\xi_0\}],$$

$$K_{33}^* = \frac{1}{4 r_3 r_4}$$
$$\cdot[+ A_m^*\{r_3 \operatorname{Sinh}\beta_3\xi_0 \operatorname{Cos}\beta_4\xi_0 - r_4 \operatorname{Cosh}\beta_3\xi_0 \operatorname{Sin}\beta_4\xi_0\}$$
$$+ B_m^*\{r_3 \operatorname{Sinh}\beta_3\xi_0 \operatorname{Sin}\beta_4\xi_0 + r_4 \operatorname{Cosh}\beta_3\xi_0 \operatorname{Cos}\beta_4\xi_0\} \tag{53}$$
$$+ C_m^*\{r_3 \operatorname{Cosh}\beta_3\xi_0 \operatorname{Cosh}\beta_4\xi_0 - r_4 \operatorname{Sinh}\beta_3\xi_0 \operatorname{Sin}\beta_4\xi_0\}$$
$$+ D_m^*\{r_3 \operatorname{Cosh}\beta_3\xi_0 \operatorname{Sin}\beta_4\xi_0 + r_4 \operatorname{Sinh}\beta_3\xi_0 \operatorname{Cos}\beta_4\xi_0\}],$$

$$K_{43}^* = \frac{1}{4 r_3 r_4}$$
$$\cdot[+ A_m^*\{(r_3^3 - 3 r_3 r_4^2)\operatorname{Sinh}\beta_3\xi_0 \operatorname{Cos}\beta_4\xi_0 + (r_4^3 - 3 r_4 r_3^2)\operatorname{Cosh}\beta_3\xi_0 \operatorname{Sin}\beta_4\xi_0\}$$
$$+ B_m^*\{(r_3^3 - 3 r_3 r_4^2)\operatorname{Sinh}\beta_3\xi_0 \operatorname{Sin}\beta_4\xi_0 - (r_4^3 - 3 r_4 r_3^2)\operatorname{Cosh}\beta_3\xi_0 \operatorname{Cos}\beta_4\xi_0\} \tag{54}$$
$$+ C_m^*\{(r_3^3 - 3 r_3 r_4^2)\operatorname{Cosh}\beta_3\xi_0 \operatorname{Cos}\beta_4\xi_0 + (r_4^3 - 3 r_4 r_3^2)\operatorname{Sinh}\beta_3\xi_0 \operatorname{Sin}\beta_4\xi_0\}$$
$$+ D_m^*\{(r_3^3 - 3 r_3 r_4^2)\operatorname{Cosh}\beta_3\xi_0 \operatorname{Sin}\beta_4\xi_0 - (r_4^3 - 3 r_4 r_3^2)\operatorname{Sinh}\beta_3\xi_0 \operatorname{Cos}\beta_4\xi_0\}].$$

The dimensionless parameters used are as follows:

$$\beta_3 = \alpha_n b r_3 = \frac{n\pi b}{L}\sqrt{\frac{\sqrt{\frac{D_x}{D_y}} + \frac{H}{D_y}}{2}} \tag{55}$$

and

$$\beta_4 = \alpha_n b r_4 = \frac{n\pi b}{L}\sqrt{\frac{\sqrt{\frac{D_x}{D_y}} - \frac{H}{D_y}}{2}}. \tag{56}$$

The parameters ξ_0, ξ_1 and ψ are the same as in case 1. The upper and lower signs of K_{33}^* and K_{43}^* are for stations to the right and left of the load respectively.

The constants used are

$$A_m^* = \frac{(S_{13}^* + S_{23}^*)\, d_{33} - (S_{33}^* - S_{43}^*)\, d_{13}}{2\,(a_{13}\, d_{33} - a_{33}\, d_{13})}, \tag{57a}$$

$$B_m^* = \frac{(S_{13}^* - S_{23}^*)\, c_{33} - (S_{33}^* + S_{43}^*)\, c_{13}}{2\,(b_{13}\, c_{33} - c_{13}\, b_{33})}, \tag{57b}$$

$$C_m^* = \frac{(S_{33}^* + S_{43}^*)\, b_{13} - (S_{13}^* - S_{23}^*)\, b_{33}}{2\,(b_{13}\, c_{33} - c_{13}\, b_{33})}, \tag{57c}$$

$$D_m^* = \frac{(S_{33}^* - S_{43}^*)\, a_{13} - (S_{13}^* + S_{23}^*)\, a_{33}}{2\,(a_{13}\, d_{33} - a_{33}\, d_{13})}, \tag{57d}$$

where

$$\begin{aligned} S_{13}^* = \frac{1}{(r_3^2 + r_4^2)} \Bigg[& \left\{ G\, J\, \alpha_n - \frac{r_3\,[D_2 - D_y\,(r_3^2 + r_4^2)]}{(r_3^2 + r_4^2)} \right\} \\ & \cdot \{ [r_3 \operatorname{Sin} \beta_4 (\eta_1 - \psi) + r_4 \operatorname{Cos} \beta_4 (\eta_1 + \psi)]\, e^{-\beta_3 (\eta_1 - \psi)} \\ & - [r_3 \operatorname{Sin} \beta_4 (\eta_1 + \psi) + r_4 \operatorname{Cos} \beta_4 (\eta_1 + \psi)\, e^{-\beta_3 (\eta_1 + \psi)} \} \\ & - \left\{ \frac{r_4\,[D_2 + D_y\,(r_3^2 + r_4^2)]}{(r_3^2 + r_4^2)} \right\} \\ & \cdot \{ [r_3 \operatorname{Cos} \beta_4 (\eta_1 - \psi) - r_4 \operatorname{Sin} \beta_4 (\eta_1 - \psi)]\, e^{-\beta_3 (\eta_1 - \psi)} \\ & - [r_3 \operatorname{Cos} \beta_4 (\eta_1 + \psi) - r_4 \operatorname{Sin} \beta_4 (\eta_1 + \psi)\, e^{-\beta_3 (\eta_1 + \psi)} \} \Bigg], \end{aligned} \tag{58a}$$

$$\begin{aligned} S_{23}^* = \frac{1}{(r_3^2 + r_4^2)} \Bigg[& \left\{ G\, J\, \alpha_n - \frac{r_3\,[D_2 - D_y\,(r_3^2 + r_4^2)]}{(r_3^2 + r_4^2)} \right\} \\ & \cdot \{ [r_3 \operatorname{Sin} \beta_4 (\eta_2 - \psi) + r_4 \operatorname{Cos} \beta_4 (\eta_2 - \psi)]\, e^{-\beta_3 (\eta_2 - \psi)} \\ & - [r_3 \operatorname{Sin} \beta_4 (\eta_2 + \psi) + r_4 \operatorname{Cos} \beta_4 (\eta_2 + \psi)]\, e^{-\beta_3 (\eta_2 + \psi)} \} \\ & - \left\{ \frac{r_4\,[D_2 + D_y\,(r_3^2 + r_4^2)]}{(r_3^2 + r_4^2)} \right\} \\ & \cdot \{ [r_3 \operatorname{Cos} \beta_4 (\eta_2 - \psi) - r_4 \operatorname{Sin} \beta_4 (\eta_2 - \psi)]\, e^{-\beta_3 (\eta_2 - \psi)} \\ & - [r_3 \operatorname{Cos} \beta_4 (\eta_2 + \psi) - r_4 \operatorname{Sin} \beta_4 (\eta_2 + \psi)]\, e^{-\beta_3 (\eta_2 + \psi)} \} \Bigg], \end{aligned} \tag{58b}$$

$$\begin{aligned} S_{33}^* = \frac{1}{(r_3^2 + r_4^2)^2} & [\{ [D_y\,(r_4^2 - r_3^2) + D_2 + D_{xy} + D_{yx}]\,(r_3^2 + r_4^2) - E\, I\, \alpha_n\, r_3 \} \\ & \cdot \{ [r_3 \operatorname{Sin} \beta_4 (\eta_1 - \psi) + r_4 \operatorname{Cos} \beta_4 (\eta_1 - \psi)]\, e^{-\beta_3 (\eta_1 - \psi)} \\ & - [r_3 \operatorname{Sin} \beta_4 (\eta_1 + \psi) + r_4 \operatorname{Cos} \beta_4 (\eta_1 + \psi)]\, e^{-\beta_3 (\eta_1 + \psi)} \} \\ & + \{ 2\, D_y\, r_3\, r_4\, (r_3^2 + r_4^2) - E\, I\, \alpha_n\, r_4 \} \\ & \cdot \{ [r_3 \operatorname{Cos} \beta_4 (\eta_1 - \psi) - r_4 \operatorname{Sin} \beta_4 (\eta_1 - \psi)]\, e^{-\beta_3 (\eta_1 - \psi)} \\ & - [r_3 \operatorname{Cos} \beta_4 (\eta_1 + \psi) - r_4 \operatorname{Sin} \beta_4 (\eta_1 + \psi)]\, e^{-\beta_3 (\eta_1 + \psi)} \}], \end{aligned} \tag{58c}$$

$$
\begin{aligned}
S^*_{43} = \frac{1}{(r_3^2+r_4^2)^2}\,&[\{E\,I\,\alpha_n\,r_4 - 2\,D_y\,r_3\,r_4\,(r_3^2+r_4^2)\}\\
&\cdot\{[r_3\,\mathrm{Cos}\,\beta_4\,(\eta_2-\psi) - r_4\,\mathrm{Sin}\,\beta_4\,(\eta_2-\psi)]\,e^{-\beta_3(\eta_2-\psi)}\\
&-[r_3\,\mathrm{Cos}\,\beta_4\,(\eta_2+\psi) - r_4\,\mathrm{Sin}\,\beta_4\,(\eta_2+\psi)]\,e^{-\beta_3(\eta_2+\psi)}\}\\
&+\{E\,I\,\alpha_n\,r_3 - (r_3^2+r_4^2)\,[D_y\,(r_4^2-r_3^2) + D_2 + D_{xy} + D_{yx}]\}\\
&\cdot\{[r_3\,\mathrm{Sin}\,\beta_4\,(\eta_2-\psi) + r_4\,\mathrm{Cos}\,\beta_4\,(\eta_2-\psi)]\,e^{-\beta_3(\eta_2-\psi)}\\
&-[r_3\,\mathrm{Sin}\,\beta_4\,(\eta_2+\psi) + r_4\,\mathrm{Cos}\,\beta_4\,(\eta_2+\psi)]\,e^{-\beta_3(\eta_2-\psi)}\}],
\end{aligned}
\tag{58d}
$$

$$
\begin{aligned}
a_{13} = {}&[D_2 - D_y\,(r_3^2-r_4^2)]\,\mathrm{Cosh}\,\beta_3\,\mathrm{Cos}\,\beta_4 + 2\,D_y\,r_3\,r_4\,\mathrm{Sinh}\,\beta_3\,\mathrm{Sin}\,\beta_4\\
&+ G\,J\,\alpha_n\,(r_3\,\mathrm{Sinh}\,\beta_3\,\mathrm{Cos}\,\beta_4 - r_4\,\mathrm{Cosh}\,\beta_3\,\mathrm{Sin}\beta_4),
\end{aligned}
\tag{59a}
$$

$$
\begin{aligned}
b_{13} = {}&[D_2 - D_y\,(r_3^2-r_4^2)]\,\mathrm{Cosh}\,\beta_3\,\mathrm{Sin}\,\beta_4 - 2\,D_y\,r_3\,r_4\,\mathrm{Sinh}\,\beta_3\,\mathrm{Cos}\,\beta_4\\
&+ G\,J\,\alpha_n\,(r_3\,\mathrm{Sinh}\,\beta_3\,\mathrm{Sin}\,\beta_4 + r_4\,\mathrm{Cosh}\,\beta_3\,\mathrm{Cos}\,\beta_4),
\end{aligned}
\tag{59b}
$$

$$
\begin{aligned}
c_{13} = {}&[D_2 - D_y\,(r_3^2-r_4^2)]\,\mathrm{Sinh}\,\beta_3\,\mathrm{Cos}\,\beta_4 + 2\,D_y\,r_3\,r_4\,\mathrm{Cosh}\,\beta_3\,\mathrm{Sin}\,\beta_4\\
&+ G\,J\,\alpha_n\,(r_3\,\mathrm{Cosh}\,\beta_3\,\mathrm{Cos}\,\beta_4 - r_4\,\mathrm{Sinh}\,\beta_3\,\mathrm{Sin}\,\beta_4),
\end{aligned}
\tag{59c}
$$

$$
\begin{aligned}
d_{13} = {}&[D_2 - D_y\,(r_3^2-r_4^2)]\,\mathrm{Sinh}\,\beta_3\,\mathrm{Sin}\,\beta_4 - 2\,D_y\,r_3\,r_4\,\mathrm{Cosh}\,\beta_3\,\mathrm{Cos}\,\beta_4\\
&+ G\,J\,\alpha_n\,(r_3\,\mathrm{Cosh}\,\beta_3\,\mathrm{Sin}\,\beta_4 + r_4\,\mathrm{Sinh}\,\beta_3\,\mathrm{Cos}\,\beta_4),
\end{aligned}
\tag{59d}
$$

$$
\begin{aligned}
a_{33} = {}&[r_3\,(D_2 + D_{xy} + D_{yx}) - D_y\,(r_3^3 - 3\,r_3\,r_4^2)]\,\mathrm{Sinh}\,\beta_3\,\mathrm{Cos}\,\beta_4\\
&-[r_4\,(D_2 + D_{xy} + D_{yx}) + D_y\,(r_4^3 - 3\,r_4\,r_3^2)]\,\mathrm{Cosh}\,\beta_3\,\mathrm{Sin}\,\beta_4\\
&+ E\,I\,\alpha_n\,\mathrm{Cosh}\,\beta_3\,\mathrm{Cos}\,\beta_4,
\end{aligned}
\tag{59e}
$$

$$
\begin{aligned}
b_{33} = {}&[r_3\,(D_2 + D_{xy} + D_{yx}) - D_y\,(r_3^3 - 3\,r_3\,r_4^2)]\,\mathrm{Sinh}\,\beta_3\,\mathrm{Sin}\,\beta_4\\
&+[r_4\,(D_2 + D_{xy} + D_{yx}) + D_y\,(r_4^3 - 3\,r_4\,r_3^2)]\,\mathrm{Cosh}\,\beta_3\,\mathrm{Cos}\,\beta_4\\
&+ E\,I\,\alpha_n\,\mathrm{Cosh}\,\beta_3\,\mathrm{Sin}\,\beta_4,
\end{aligned}
\tag{59f}
$$

$$
\begin{aligned}
c_{33} = {}&[r_3\,(D_2 + D_{xy} + D_{yx}) - D_y\,(r_3^3 - 3\,r_3\,r_4^2)]\,\mathrm{Cosh}\,\beta_3\,\mathrm{Cos}\,\beta_4\\
&-[r_4\,(D_2 + D_{xy} + D_{yx}) + D_y\,(r_4^3 - 3\,r_4\,r_3^2)]\,\mathrm{Sinh}\,\beta_3\,\mathrm{Sin}\,\beta_4\\
&+ E\,I\,\alpha_n\,\mathrm{Sinh}\,\beta_3\,\mathrm{Cos}\,\beta_4,
\end{aligned}
\tag{59g}
$$

$$
\begin{aligned}
d_{33} = {}&[r_3\,(D_2 + D_{xy} + D_{yx}) - D_y\,(r_3^3 - 3\,r_3\,r_4^2)]\,\mathrm{Cosh}\,\beta_3\,\mathrm{Sin}\,\beta_4\\
&+[r_4\,(D_2 + D_{xy} + D_{yx}) + D_y\,(r_4^3 - 3\,r_4\,r_3^2)]\,\mathrm{Sinh}\,\beta_3\,\mathrm{Cos}\,\beta_4\\
&+ E\,I\,\alpha_n\,\mathrm{Sinh}\,\beta_3\,\mathrm{Sin}\,\beta_4.
\end{aligned}
\tag{59h}
$$

Similar equations for isotropic and articulated bridge decks have been derived but are not included here. The isotropic case can be obtained from Case 1 by means of a digital computer, setting $H = 1.0001$ and $D_x = D_y = 1$. By assuming a value of $H = 0.9999$ and $D_x = D_y = 1$, the isotropic case can also be obtained from Case 3. When this is done the three results coincide,

providing a good check of the solutions and confirming the continuity of the functions from $H^2 > D_x D_y$ to $H^2 < D_x D_y$ with the isotropic case as the dividing line. The case of the articulated bridge deck may be obtained by computer from Case 1 by setting a very small value for D_y (say $0.0001\, D_x$) and not zero. The results check very favourably with the exact solution for the special case where D_y is zero.

Another check was made on the validity of the equations by allocating a very small value to the dimensions of the rectangular load u and v (about $0.0001\, b$) and the results coincide with those for concentrated loads [5].

Examining the equations for deflection, it is apparent that the convergence of the series is controlled by $1/n^5$ and as such converges rapidly compared with $1/n^3$ for concentrated loads. With this convergence, the first harmonic gives values sufficiently accurate for design purposes. The equations for longitudinal, transverse and twisting moments are controlled by the term $1/n^3$ and again, even the first harmonic will be sufficient for preliminary design. Shearing and reactive forces converge as a function of $1/n^2$ and a few harmonics only will be needed to obtain reliable results. This is a considerable improvement on the present equations based on concentrated loads where the expressions for moments, shears and reactive forces do not converge rapidly.

The present analysis incorporates the flexural and torsional rigidities of the edge-stiffening beams at the edges of the deck. If these beams are not present, $E\,I$ and $G\,J$ are set to zero. Using these edge beam rigidities, equations for different boundary conditions at the edges of the bridge may be obtained for the analysis not only of bridge decks, but also of orthotropic floor slabs.

Discussion and Conclusions

The expressions for deflection, moments, shears and reactive forces may be conveniently presented in the form of a dimensionless distribution coefficient which may be defined as the ratio of the actual value to the mean value at that transverse section.

For example, the mean deflection at a section distance x from the support due to a patch load of length $2\,u$ whose centre is at a distance c from the support may be written as

$$w_{mean} = \frac{W L^4}{u\, b\, \pi^5 D_x} \sum_{n=1}^{\infty} \frac{1}{n^5} \operatorname{Sin} \alpha_n u \operatorname{Sin} \alpha_n c \operatorname{Sin} \alpha_n x \tag{60}$$

and the distribution coefficient for deflection may be expressed as

$$K \text{ (for deflection)} = \frac{b}{v} \frac{\sum_{n=1}^{\infty} \frac{1}{n^5} \operatorname{Sin} \alpha_n u \operatorname{Sin} \alpha_n c \operatorname{Sin} \alpha_n x \,(K_1^*)}{\sum_{n=1}^{\infty} \frac{1}{n^5} \operatorname{Sin} \alpha_n u \operatorname{Sin} \alpha_n c \operatorname{Sin} \alpha_n x} \tag{61}$$

and since the series converges rapidly, the distribution coefficient for deflection considering the first harmonic only is

$$K \text{ (for deflection)} = \frac{b}{v} K_1^*. \tag{62}$$

The case of concentrated load acting on the deck may be obtained from Eq. (62) by studying the limit of $\frac{b}{v} K_1^*$ as u and v approach zero and it may be shown that

$$\lim_{\substack{u \to 0 \\ v \to 0}} \left(\frac{b}{v} K_1^*\right) = (K_{11}, K_{12} \text{ or } K_{13}), \tag{63}$$

where K_{11}, K_{12} and K_{13} are defined in Eq. (4).

Similarly, for longitudinal and transverse moments, the distribution coefficients may be written as

$$K \text{ (for } M_x) = \frac{b}{v} \frac{\sum_{n=1}^{\infty} \frac{1}{n^3} \operatorname{Sin} \alpha_n u \operatorname{Sin} \alpha_n c \operatorname{Sin} \alpha_n x \left(K_1^* - \frac{D_1}{D_x} K_2^*\right)}{\sum_{n=1}^{\infty} \frac{1}{n^3} \operatorname{Sin} \alpha_n u \operatorname{Sin} \alpha_n c \operatorname{Sin} \alpha_n x}, \tag{64}$$

$$K \text{ (for } M_y) = -\frac{b}{v} \frac{\sum_{n=1}^{\infty} \frac{1}{n^3} \operatorname{Sin} \alpha_n u \operatorname{Sin} \alpha_n c \operatorname{Sin} \alpha_n x \left(\frac{D_y}{D_x} K_2^* - \frac{D_2}{D_x} K_1^*\right)}{\sum_{n=1}^{\infty} \frac{1}{n^3} \operatorname{Sin} \alpha_n u \operatorname{Sin} \alpha_n c \operatorname{Sin} \alpha_n x}. \tag{65}$$

Note that in Eq. (65) the distribution coefficient for transverse moment is the ratio of the transverse moment M_y to the mean longitudinal moment M_x. A similar case holds true for twisting moments M_{xy} and M_{yx}, thus

$$K \text{ (for } M_{xy}) = \frac{b}{v} \frac{L}{\pi} \frac{\sum_{n=1}^{\infty} \frac{1}{n^3} \operatorname{Sin} \alpha_n u \operatorname{Sin} \alpha_n c \operatorname{Cos} \alpha_n x \left(\frac{D_{xy}}{D_y} K_3^*\right)}{\sum_{n=1}^{\infty} \frac{1}{n^2} \operatorname{Sin} \alpha_n u \operatorname{Sin} \alpha_n c \operatorname{Cos} \alpha_n x}. \tag{66}$$

Two examples are shown in Fig. 3 to illustrate the effect of rectangular patch loads on orthotropic bridge decks. The decks are square in plan and one was chosen with torsional parameter $\alpha < 1$ and the other with $\alpha > 1$. The patch load covers 10% of the width of the deck (i.e. $\psi = v/b = 0.10$). Central and eccentric load positions are shown for each case. The curves are presented in the form dimensionless distribution coefficients for deflection K defined by Eq. (61).

The theory as presented provides a logical and effective method of predicting the distribution of rectangular patch loads on an orthotropic deck with or without edge stiffening beams. With these equations, it is possible to

analyze all types of orthotropic bridge decks from the torsionless type to the articulated plate. It has been shown theoretically that by dissipating the load over a finite rectangular area, the problem of convergence is overcome and the theoretical results are accurate even if the first harmonic of the series only is used.

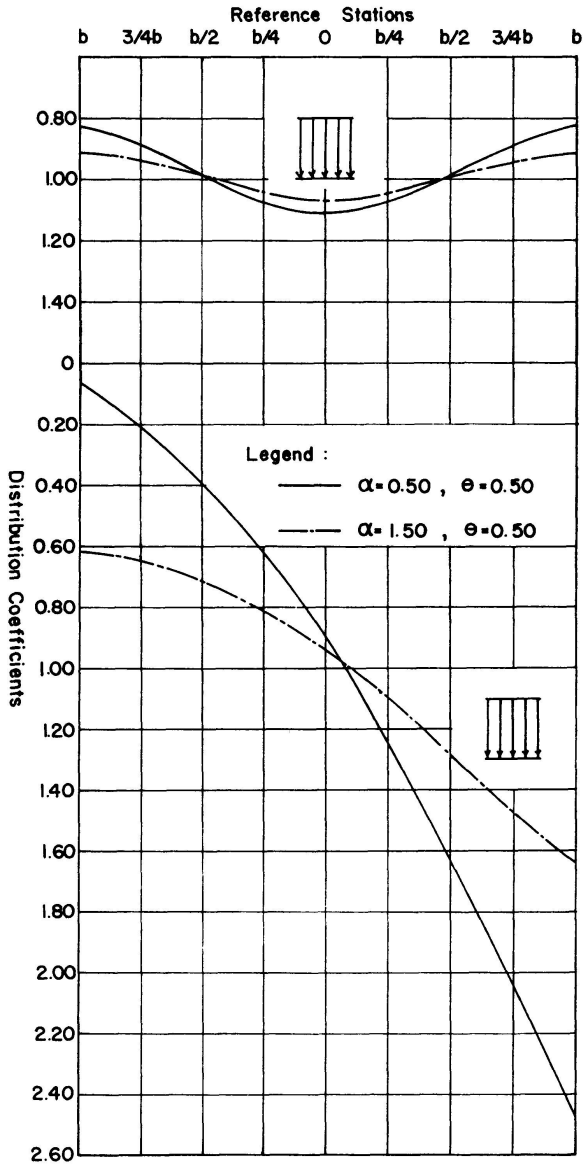

Fig. 3. Transverse profiles of torsionally soft-flexurally stiff and torsionally stiff-flexurally soft bridge decks under central and eccentric patch load with $\Psi = 0.10$.

Summing up, this paper has presented equations for finding the deflections, bending and torsional moments, and shearing and reactive forces due to rectangular patch loads acting on simply supported orthotropic bridge decks classified according to their relative rigidities in flexure and torsion. The

application of the theory necessitates an accurate and reliable method of determining the flexural and torsional rigidities of the deck and further investigation both experimental and theoretical is required.

References

1. Huber, M. T.: Die Theorie der kreuzweise bewehrten Eisenbetonplatte nebst Anwendungen auf mehrere bautechnisch wichtige Aufgaben über Rechteckplatten. Der Bauingenieur, Berlin, 1923.
2. Guyon, Y.: Calcul des ponts larges à poutres multiples solidarisées par des entretoises. Annales des Ponts et Chaussées, Paris, 1946.
3. Massonnet, C.: Methode de calcul des ponts à poutres multiples tenant compte de leur resistance à la torsion. Publications, International Association for Bridge and Structural Engineering, Vol. 10, Zurich, 1950.
4. Pama, R. P. and Cusens, A. R.: Load Distribution in Multibeam Concrete Bridges. Paper presented to the International Symposium on Concrete Bridge Design held at Toronto, Canada, April 1967.
5. Cusens, A. R. and Pama, R. P.: The Distribution of Concentrated Load on Orthotropic Bridge Decks. The Structural Engineer, Vol. 47, No. 9, Sept. 1969.
6. Spindel, J. E.: A Study of Bridge Slabs Having no Transverse Flexural Stiffness. Thesis presented to the University of London, in 1961, in partial fulfilment of the requirements for the degree Doctor of Philosophy.
7. Morice, P. B., Little, G. and Rowe, R. E.: Design Curves for the Effect of Concentrated Loads on Concrete Bridge Decks. Cement and Concrete Association, July 1956.

Summary

The paper presents the analysis of simply supported orthotropic bridge decks due to rectangular patch loads. The deck is classified into three main categories depending on their relative rigidities in flexure and torsion. Series solutions were employed to determine the expressions for deflection, bending and torsional moments, shearing and reactive forces.

Résumé

Ce rapport présente l'analyse des effets de charges concentrées sur les ponts orthotropes simples. Les plaques sont réparties en trois catégories principales suivant leur rigidité à la flexion et à la torsion.

Les expressions du fléchissement, des moments de flexion et de torsions, des efforts tranchants et des réactions furent déterminées à l'aide des séries.

Zusammenfassung

Der Beitrag zeigt die Berechnung einfach aufgelegter orthotroper Brückenplatten unter Radlasten. Die Platte ist in drei Hauptklassen eingeteilt, die von der relativen Biege- und Drillsteifigkeit abhängen. Reihenentwicklungen sind zur Bestimmung der Durchbiegung, der Biege- und Drillmomente, Quer- und Auflagerkräfte angewandt worden.